Thermal Conductivity of Aqueous $Mg(NO_3)_2$, $Ca(NO_3)_2$, and $Ba(NO_3)_2$ Solutions at High Temperatures and High Pressures

Lala A. Akhmedova-Azizova*

Azerbaijan State Oil Academy, Baku, AZ1010, Azerbaijan

Thermal conductivity of four aqueous $Mg(NO_3)_2$ solutions of molality (0.7507, 1.689, 2.895, and 4.5040) mol·kg^{-1}, four aqueous $Ca(NO_3)_2$ solutions of molality (0.6771, 1.5235, 2.598, and 4.063) mol·kg^{-1}, and $Ba(NO_3)_2$ (0.0781, 0.1594, 0.2442, and 0.3327) mol·kg^{-1} have been measured with a concentric-cylinder (steady-state) technique. Measurements were made at five isobars (0.1, 10. 20, 30, and 40) MPa for H_2O + $Mg(NO_3)_2$, H_2O + $Ca(NO_3)_2$, and H_2O + $Ba(NO_3)_2$ solutions. The range of temperature was (293.15 to 591.06) K. The total uncertainty of thermal conductivity, pressure, temperature, and molality measurements was estimated to be less than 2 %, 0.05 %, 30 mK, and 0.02 %, respectively. The measured values of thermal conductivity were compared with data and correlations reported in the literature. The reliability and accuracy of the experimental method was confirmed with measurements on pure water, toluene, and H_2O + NaCl with well-known thermal conductivity values. The experimental and calculated values of thermal conductivity for pure water from IAPWS formulation show excellent agreement within their experimental uncertainties (AAD within 0.44 %) in the temperature range from (308.4 to 704.2) K and at pressures up to 60 MPa. Correlation equations for thermal conductivity of the solutions studied were obtained as a function of temperature, pressure, and composition by a least-squares method from the experimental data. The AAD between measured and calculated values from this correlation equation for the thermal conductivity was (0 to 0.7) %.

Introduction

Transport properties of aqueous solutions over a wide range of temperatures and concentrations are needed in many industrial and scientific applications such as calculation of design parameters, developments and utilization of geothermal and ocean thermal energy, efficient operation of high-temperature energy-generating systems, geology and mineralogy, for hydrothermal synthesis, and biological processes of living organisms. Oceans and underground waters and the largest reservoirs of aqueous electrolyte solutions NO_3^- are important components of natural fluids, and knowledge of their aqueous solution properties is important in understanding various geochemical processes (such as seafloor vents and geothermal energy production) related to subsurface brines and mineral scaling harms. Because of the lack of reliable experimental information on thermal conductivity of aqueous solutions, the design parameters are often obtained empirically.

A database of thermal conductivity in high-temperature aqueous systems is needed to support the advancement of theoretical work. Better predictive models should be developed on basic reliable experimental information on thermodynamic and transport properties data. However, measurements of the thermal conductivity of aqueous salt solutions have so far been limited to rather narrow ranges of temperature, pressure, and concentration with less satisfactory accuracy.

The main objective of this paper is to provide new accurate experimental thermal conductivity data for aqueous $Mg(NO_3)_2$, $Ca(NO_3)_2$, and $Ba(NO_3)_2$ solutions at high temperatures (up to 591.06) K and high pressures (up to 40) MPa. This work is a part of a continuing program on the transport properties of electrolytes in aqueous solutions. In previous studies,[1−9] we measured the thermal conductivity of 25 aqueous salt solutions at high temperatures (up to 573.15) K and high pressures (up to 100) MPa. Some of the reported thermal conductivities are inaccurate and inconsistent.

* E-mail: lakhmedovaaz@mail.ru.

Experimental Procedures

Apparatus and Construction of the Thermal Conductivity Cell. The thermal conductivity of aqueous $Mg(NO_3)_2$, $Ca(NO_3)_2$, and $Ba(NO_3)_2$ solutions was measured by a concentric-cylinders (steady-state) technique. The experimental apparatus and procedures that were described previously[1−3,6] were used without modification. In this paper, only a brief discussion will be given.

The main part of the apparatus consisted of a high-pressure autoclave, thermostat, and thermal conductivity cell. The thermal conductivity cell consisted of two coaxial cylinders: an inner (emitting) cylinder and an outer (receiving) cylinder. The cylinders were located in a high-pressure autoclave. The deviation from concentricity was 0.002 cm or 2 % of the sample layer.

The autoclave was located in the thermostat. The thermostat was a solid (massive) copper block. The temperature in the thermostat was controlled with a heater.

The thermostat was supplied with a three-section heating element, PRT-10, and three chromel−alumel thermocouples were located on three different levels of the copper block. The temperature differences between various sections (levels) of the copper block were within 0.02 K of each other. Temperature was measured with a PRT and with three chromel−alumel thermocouples. Thermocouples were located of different levels of the thermostat to minimize temperature inhomogeneities. One of the junctions of a differential chromel−copel thermocouple was located in the inner cylinder and was tightly applied to the cylinder's wall. The second junction of the thermocouple was

10.1021/je050393n CCC: $33.50
Published on Web 02/11/2006

located in the shell capillary. Thermocouples were twice calibrated with a standard resistance thermometer. The difference between calibrations was 10 mK. The reading of the single thermocouple differs by ± 10 mK. The measurements were started when the differences in the readings of all of the thermocouples were minimal (0.02 K).

Geometrical Characteristics of the Thermal Conductivity Cell. The important dimensions of the thermal conductivity cell are outside diameter of the inner cylinder is $d_2 = (10.98 \pm 0.01) \times 10^{-3}$ m and inner diameter of the outer cylinder is $d_1 = (12.92 \pm 0.02) \times 10^{-3}$ m. The length of the measuring section of the inner cylinder (emitter) is $l = (150 \pm 0.1) \times 10^{-3}$ m. The gap between cylinders (thickness of the liquid gap) was $d = (0.97 \pm 0.03) \times 10^{-3}$ m. The choice of this gap was a compromise between decreasing convection and accommodation effect. The acceptable value for the thickness of the liquid layer d is between 0.5 and 1 mm. If $d > 1$ mm, the natural convection heat transfer will develop. The optimal value ratio of the length l to the diameter of the inner cylinder d_2 should be $l/d_2 = 10$ to 15. It is very difficult to keep the homogeneity of the temperature distribution along the length of inner cylinder when the ratio $l/d_2 > 15$. If $l/d_2 < 10$, the influence of the end effect is significant.

The solution under investigation is confined in the vertical gap of the cell. Pressure in the system was created and measured with piston manometers MP-600 and MP-60 with upper limits measurement of 600 bar and 60 bar, respectively. In the cell, heat was generated in the microheater that consists of an isolated (high-temperature lacquer-covered) constantan wire of 0.1 mm diameter. A microheater was mounted inside the inner cylinder (emitter), which was closely wound around a surface of a 2 mm diameter ceramic tube and isolated with high-temperature lacquer. The tube is tightly fitted in the heater pocket with a diameter of 6 mm on the inner cylinder. All heaters were made with 0.1 mm diameter constantan wire and isolated with high-temperature lacquer.

The electrical schema of the measurements consists of circuits of PRT, calorimetric heater, and differential and single thermocouples. All electrical measurements were performed with the compensation method using direct-current semiautomatic potentiometers (P323/2).

Principles of Operation, Working Equation, and Corrections. With this method, the heat generated in an inner emitting cylinder is conducted radially through the narrow fluid-filled annulus to a coaxial receiving cylinder. In this method, the thermal conductivity λ of the fluid was deduced from measurements of heat Q transmitted across the solution layer, the temperature difference ΔT between the inner and outer cylinders, the thickness of the solution layer d, and effective length l of measuring part of the cylinder (effective length of the cylinders).

After taking into account all corrections, we can write the final working equation for the thermal conductivity as

$$\lambda = A\frac{Q_{\text{meas}} - Q_{\text{los}}}{\Delta T_{\text{meas}} - \Delta T_{\text{corr}}} \tag{1}$$

where $A = \ln(d_2/d_1)/2\pi l$ is the geometric constant that can be determined with geometrical characteristics of the experimental cell; Q_{mens} is the amount of heat released by the calorimetric microheater; Q_{los} is the amount of heat lost through the ends of the measuring cell (end effect); $\Delta T_{\text{corr}} = \Delta T_{\text{cl}} + \Delta T_{\text{lac}}$; ΔT_{cl} and ΔT_{lac} are the temperature differences in the cylinder walls and lacquer coat, respectively; ΔT_{meas} is the temperature difference measured with differential thermocouples. The values of A can be also determined by means of a calibration technique using thermal conductivity data for the reference fluid (pure water, IAPWS[10]). The values of the cell constant determined both with geometrical characteristics of the experimental cell and by calibration techniques (pure water at temperature 293.15 K) are 0.1727 m^{-1} and 0.1752 m^{-1}, respectively. In this work, we used the value of A as a function of temperature derived using calibration procedure with pure water (IAPWS[10]). The geometrical constant A changes by 12 % over the temperature range from (293.15 to 750.15) K. The change in the cell size due to pressure was considered negligible due to the low volume compressibility of stainless steel (1XI8H9T).

Because of the large emitter size and the small fluid volume surrounding the emitter, no effect of accommodation was to be expected. The calibration of the cell was made at a pressure of 60 MPa to avoid corrections due to accommodation effect.

It is difficult to estimate the values of Q_{los} and ΔT_{corr} by calculation. In this work, the values of Q_{los} and ΔT_{corr} were estimated by measuring standard liquids (water) with well-known thermal conductivity (IAPWS[10] standard). Calibration was made with pure water at 10 selected temperatures between (293.15 and 713.15) K and at three selected pressures between (0.1 and 60) MPa. The amount of heat flow Q and the temperature difference ΔT were 13.06 W and 3.5 K, respectively. The estimated value of Q_{los} is about 0.05 W. This value is negligible (0.38 %) by comparison with the heat transfer by conduction $Q = 13.06$ W.

Convection Heat Transfer. Convection heat transfer increases with increasing values of the Rayleigh number (Ra). To reduce the values of Ra, a small gap distance between cylinders $d = (0.97 \pm 0.03) \times 10^{-3}$ m was used. This makes it possible to minimize the risk of convection. Convection could develop when the Ra exceeds a certain critical value Ra_c, which for vertical coaxial cylinders is about 1000 (Gershuni[11]). Therefore, $Ra > 1000$ was considered as a criterion for the beginning of convection. In the range of the present experiments, the values of Ra were always less than 500, and Q_{con} is estimated to be negligibly small. The absence of convection can be verified experimentally by measuring the thermal conductivity with different temperature differences ΔT across the measurement gap and different power Q transferred from the inner to the outer cylinder. The measured thermal conductivity was indeed independent of the applied temperature differences ΔT and power Q transferred from the inner to outer cylinder.

Heat Transfer by Radiation. Any conductive heat transfer must be accompanied by simultaneous radiative transfer. The correction depends on whether the fluid absorbs radiation. If the fluid is entirely transparent, then the conductive and radiative heat fluxes are additive and independent, and the simple correction given by Healy et al.[12] is adequate and usually negligible. When the fluid absorbs and re-emits radiation (partially transparent), the problem is more complicated since then the radiative and conductive fluxes are coupled. In this case, effect heat transferred by radiation can be derived from the solution integro-differential equation describing coupled radiation and conduction. The approximate solution indicates that the magnitude of radiative contribution to the heat flux depends on the characteristic of the fluid for radiative absorption. The inner and outer cylinders were perfectly polished with powder of a successively smaller grain size (320 nm), their emissivity ($e = 0.32$) was small, and heat flux arising from radiation Q_{rad} is negligible by comparison with the heat transfer by conduction in the temperature range of our experiment. To minimize the heat transfer by radiation, the solid material (stainless steel 1X18H9T) of low emissivity was used for the

Table 1. Comparison between Experimental Thermal Conductivity Data and Values Calculated with IAPWS[10] Standard for Pure Water (AAD = 0.44 %)

	P/MPa = 0.1		P/MPa = 10		P/MPa = 30		P/MPa = 60	
		λ/W·m^{-1}·K^{-1}		λ/W·m^{-1}·K^{-1}		λ/W·m^{-1}·K^{-1}		λ/W·m^{-1}·K^{-1}
T/K	this work	IAPWS[10]	this work	IAPWS[10]	this work	IAPWS[10]	this work	IAPWS[10]
308.4	0.621	0.624	0.630	0.628	0.640	0.637	0.655	0.651
329.2	0.648	0.650	0.655	0.655	0.660	0.664	0.675	0.678
366.5	0.671	0.677	0.681	0.682	0.686	0.693	0.706	0.708
383.3			0.685	0.687	0.695	0.698	0.713	0.715
408.3			0.689	0.690	0.702	0.702	0.719	0.720
439.5			0.686	0.685	0.695	0.699	0.717	0.719
464.5			0.678	0.675	0.694	0.691	0.710	0.714
507.9			0.645	0.645	0.672	0.665	0.695	0.693
529.7			0.625	0.621	0.642	0.645	0.680	0.676
554.7			0.587	0.585	0.620	0.616	0.658	0.652
602.3					0.542	0.538	0.590	0.592
627.3					0.490	0.487	0.557	0.553
704.2					0.158	0.162	0.415	0.416

Table 2. Experimental Thermal Conductivities, Temperatures, and Molality of $H_2O + Mg(NO_3)_2$, $H_2O + Ca(NO_3)_2$, and $H_2O + Ba(NO_3)_2$ Solutions at 0.1 MPa

$H_2O + Mg(NO_3)_2$			$H_2O + Ca(NO_3)_2$			$H_2O + Ba(NO_3)_2$		
m	T	λ	m	T	λ	m	T	λ
mol·kg^{-1}	K	W·m^{-1}·K^{-1}	mol·kg^{-1}	K	W·m^{-1}·K^{-1}	mol·kg^{-1}	K	W·m^{-1}·K^{-1}
0.705	295.98	0.587	0.6771	295.08	0.588	0.0781	294.78	0.600
0.705	313.91	0.612	0.6771	320.68	0.620	0.0781	311.12	0.627
0.705	338.12	0.636	0.6771	346.45	0.642	0.0781	334.78	0.649
0.705	352.16	0.644	1.5235	296.67	0.578	0.0781	350.46	0.664
1.689	294.16	0.570	1.5235	320.72	0.610	0.1594	295.73	0.599
1.689	314.77	0.597	1.5235	347.72	0.634	0.1594	318.30	0.629
1.689	336.77	0.619	2.598	294.68	0.569	0.1594	337.18	0.653
1.689	352.45	0.630	2.598	321.47	0.601	0.1594	358.48	0.668
2.895	293.97	0.553	2.598	345.61	0.621	0.2442	298.16	0.601
2.895	314.97	0.582	4.063	298.12	0.566	0.2442	315.58	0.625
2.895	335.34	0.604	4.063	322.29	0.593	0.2442	332.71	0.646
2.895	351.16	0.604	4.063	348.72	0.613	0.2442	361.12	0.668
4.5040	294.33	0.504				0.3327	301.12	0.599
4.5040	315.16	0.568				0.3327	317.01	0.626
4.5040	334.48	0.586				0.3327	335.67	0.645
4.5040	352.89	0.602				0.3327	359.43	0.662

cylinders, and thin layers of fluid (from 0.97 mm) are used. In this way, heat transport by radiation can be strongly reduced as compared to the heat transport by conduction. Because of the lack of characteristic optical properties of aqueous salt solutions at high temperatures, it is not possible to estimate theoretically the radiation conductivity λ_r and radiated heat Q_{rad}. The correction for absorption is small for pure water; therefore, for an aqueous solution in the temperature range up to 600 K, we assumed it to be negligible. Its influence on the uncertainty of the thermal conductivity is relatively small. The emissivity of walls was small, and Q_{rad} is negligible ($\approx$0.164 W) by comparison with the heat transfer (13.06 W) by conduction in the temperature range of our experiment.

Assessment of Uncertainties. Measurement uncertainties were associated with uncertainties that exist in measured quantities contained in working eq 1 used to compute the thermal conductivity from experimental data. The thermal conductivity was obtained from the measured quantities A, Q, T, ΔT, P, and m. The accuracy of the thermal conductivity measurements was assessed by analyzing the sensitivity of eq 1 to the experimental uncertainties of the measured quantities.

Because the uncertainties of the measured values d_1, d_2, and l are 0.15 %, 0.09 %, and 0.07 %, respectively, the corresponding uncertainty of A is 0.5 %. The experimental uncertainty of the concentration is estimated to be 0.02 %. The uncertainties of temperature end pressure measurements are $\theta_T = 0.02$ K and $\theta_P = 0.03$ MPa at a pressure of 60 MPa. The corresponding uncertainty of the thermal conductivity measurement related with uncertainties of temperature and pressure measurements is estimated to be less than 0.006 %. The uncertainty in heat flow Q measurement is about 0.1 %. To make sure that the cell was in equilibrium, the measurements were started 10 h after the time when the thermostat temperature reached the prescribed temperature. About five to six measurements are carried out at one state, and the average value of thermal conductivity is calculated. Reproducibility (scattering of the different measurements) of the measurements is about 0.5 %. From the uncertainty of the measured quantities and the corrections mentioned above, the total maximum relative uncertainty $\delta\lambda/\lambda$ in measuring the thermal conductivity was 2 %. The relative systematic uncertainty θ_λ/λ was 0.002. All of the other uncertainties were assumed negligible.

Performance Tests. To check and confirm the accuracy of the method and procedure of the measurements, thermal conductivity data were taken for pure water in the temperature range from (308.4 to 704.2) K at pressures up to 60 MPa. Table 1 provides a detailed comparison present test measurement results for pure water with the reference data for water (IAPWS[10]). Excellent agreement is found between present thermal conductivity results for pure water and the data reported by other authors (AAD within 0.2 to 1.2 %) and reference data reported by Ramires et al.[13] (AAD = 0.25 %). This excellent agreement for test measurement confirms the reliability and accuracy of the present measurements for $H_2O + Mg(NO_3)_2$,

Table 3. Experimental Thermal Conductivities, Pressures, Temperatures, and Molality of H_2O + $Mg(NO_3)_2$ Solutions

	P/MPa = 10		P/MPa = 20		P/MPa = 30		P/MPa = 40	
m	T	λ	T	λ	T	λ	T	λ
mol·kg^{-1}	K	W·m^{-1}·K^{-1}	K	W·m^{-1}·K^{-1}	K	W·m^{-1}·K^{-1}	K	W·m^{-1}·K^{-1}
0.7507	296.13	0.591	295.74	0.597	295.82	0.601	294.85	0.604
0.7507	314.31	0.616	314.91	0.623	313.98	0.628	314.02	0.632
0.7507	335.45	0.638	334.98	0.643	336.93	0.650	337.16	0.655
0.7507	357.14	0.655	358.39	0.660	359.49	0.668	357.49	0.670
0.7507	376.82	0.665	376.02	0.670	378.98	0.678	377.85	0.681
0.7507	397.12	0.672	398.14	0.677	399.12	0.684	399.82	0.688
0.7507	415.49	0.673	414.94	0.679	416.28	0.685	471.39	0.690
0.7507	431.71	0.672	432.47	0.676	433.77	0.682	432.73	0.689
0.7507	454.12	0.664	454.71	0.669	457.46	0.676	456.12	0.683
0.7507	476.38	0.652	477.73	0.658	471.08	0.668	472.83	0.677
0.7507	491.74	0.639	490.98	0.647	498.75	0.650	495.08	0.664
0.7507	517.34	0.616	517.04	0.626	513.49	0.638	512.47	0.652
0.7507	536.98	0.592	536.19	0.605	537.30	0.613	536.56	0.630
0.7507	551.14	0.568	552.98	0.584	550.17	0.598	550.18	0.614
0.7507	572.73	0.533	589.44	0.525	577.66	0.562	575.66	0.581
1.689	295.17	0.576	296.74	0.584	298.50	0.591	294.14	0.587
1.689	314.12	0.602	313.02	0.604	314.91	0.613	315.94	0.616
1.689	336.93	0.624	336.42	0.629	335.07	0.633	335.42	0.634
1.689	357.35	0.639	358.14	0.644	357.82	0.650	354.14	0.651
1.689	379.14	0.651	378.69	0.653	376.92	0.660	376.19	0.662
1.689	395.47	0.653	399.45	0.660	397.14	0.664	395.78	0.668
1.689	415.94	0.655	417.53	0.661	416.73	0.665	414.53	0.672
1.689	432.85	0.654	434.75	0.658	431.12	0.664	433.66	0.670
1.689	457.77	0.645	457.04	0.652	455.14	0.658	456.12	0.664
1.689	477.71	0.635	472.83	0.644	471.12	0.650	472.28	0.657
1.689	496.75	0.619	498.66	0.626	497.14	0.634	491.45	0.647
1.689	511.49	0.604	513.49	0.612	516.17	0.618	510.48	0.633
1.689	536.37	0.576	535.37	0.590	533.14	0.602	549.12	0.590
1.689	549.29	0.556	548.39	0.573	549.15	0.578	575.74	0.565
1.689	572.91	0.516	591.45	0.505	590.14	0.528	588.15	0.541
2.895	294.18	0.558	295.39	0.565	296.14	0.570	295.18	0.574
2.895	315.91	0.566	315.45	0.592	314.17	0.595	314.92	0.698
2.895	337.93	0.608	336.93	0.612	335.69	0.618	334.87	0.619
2.895	354.48	0.622	355.09	0.627	354.98	0.631	353.49	0.632
2.895	376.12	0.634	375.92	0.638	375.54	0.642	374.15	0.644
2.895	395.69	0.640	396.12	0.642	394.17	0.646	395.62	0.652
2.895	415.94	0.641	416.28	0.644	416.13	0.648	413.09	0.654
2.895	431.71	0.638	433.13	0.643	432.47	0.647	434.98	0.652
2.895	454.71	0.631	455.16	0.636	456.69	0.641	455.35	0.648
2.895	472.85	0.621	473.37	0.628	473.15	0.634	474.83	0.640
2.895	496.12	0.604	495.85	0.612	495.32	0.620	494.53	0.629
2.895	512.93	0.588	511.39	0.597	512.56	0.606	513.87	0.616
2.895	536.37	0.560	537.49	0.570	536.53	0.584	535.92	0.595
2.895	549.32	0.539	548.14	0.556	550.28	0.565	551.35	0.576
2.895	570.45	0.505	575.53	0.516	589.92	0.511	591.48	0.522
4.504	295.41	0.545	295.02	0.550	294.14	0.551	294.17	0.556
4.504	313.31	0.566	314.43	0.573	313.02	0.578	312.49	0.580
4.504	334.45	0.590	335.94	0.596	336.93	0.600	335.97	0.602
4.504	352.89	0.605	354.17	0.612	353.69	0.613	352.74	0.616
4.504	374.12	0.617	376.77	0.622	375.93	0.627	374.69	0.628
4.504	395.67	0.623	394.84	0.626	394.40	0.631	393.40	0.636
4.504	415.94	0.624	416.48	0.628	415.73	0.632	414.48	0.638
4.504	433.68	0.621	434.37	0.625	433.69	0.631	432.87	0.637
4.504	455.18	0.613	454.24	0.620	454.97	0.624	453.09	0.632
4.504	473.74	0.604	474.19	0.610	475.83	0.615	474.18	0.624
4.504	491.49	0.592	490.42	0.600	495.49	0.602	494.60	0.612
4.504	516.04	0.568	515.67	0.577	513.75	0.588	512.48	0.598
4.504	535.98	0.545	534.81	0.557	536.18	0.566	535.47	0.576
4.504	552.44	0.520	551.38	0.534	550.60	0.548	549.48	0.560
4.504	571.61	0.487	572.49	0.504	589.88	0.496	590.68	0.512

H_2O + $Ca(NO_3)_2$, and H_2O + $Ba(NO_3)_2$ solutions and corrects operation of the instrument.

The solutions at the desired composition were prepared by mass. The composition was checked by comparison of the density of solution at 293.15 K and 0.1 MPa with reference data.

Results and Discussion

Measurements of the thermal conductivity for four aqueous $Mg(NO_3)_2$ solutions of molality, namely, (0.7507, 1.689, 2.895, and 4.5040) mol·kg^{-1}; four aqueous $Ca(NO_3)_2$ solutions of molality (0.6771, 1.5235, 2.598, and 4.063) mol·kg^{-1}; and four aqueous $Ba(NO_3)_2$ solutions of molality (0.0781, 0.1594, 0.2442, and 0.3327) mol·kg^{-1} were performed along five isobars (0.1, 10, 20, 30, and 40) MPa between (294.11 and 591.06) K. The experimental temperature, pressure, composition, and thermal conductivity values are presented in Tables 2 to 5. The average temperature in the fluid layer equals $T_{ave} = T_1 + 0.5\Delta T$, where T_1 is the temperature of the outer cylinder and ΔT is the temperature difference across the measurement

Table 4. Experimental Thermal Conductivities, Pressures, Temperatures, and Molality of $H_2O + Ca(NO_3)_2$ Solutions

	P/MPa = 10		P/MPa = 20		P/MPa = 30		P/MPa = 40	
m	T	λ	T	λ	T	λ	T	λ
mol·kg^{-1}	K	W·m^{-1}·K^{-1}	K	W·m^{-1}·K^{-1}	K	W·m^{-1}·K^{-1}	K	W·m^{-1}·K^{-1}
0.6771	295.10	0.596	295.15	0.599	295.12	0.605	295.09	0.610
0.6771	320.70	0.628	320.71	0.632	320.70	0.638	320.68	0.642
0.6771	346.49	0.655	346.50	0.658	346.52	0.662	346.50	0.669
0.6771	372.67	0.668	372.69	0.674	372.69	0.680	372.69	0.685
0.6771	398.55	0.677	398.67	0.682	398.69	0.688	398.65	0.693
0.6771	415.03	0.676	413.09	0.683	413.12	0.690	413.15	0.695
0.6771	445.74	0.672	445.78	0.678	445.75	0.686	445.85	0.692
0.6771	470.35	0.660	470.39	0.668	470.35	0.675	470.32	0.682
0.6771	498.12	0.640	498.15	0.648	498.20	0.658	498.25	0.665
0.6771	525.54	0.610	525.61	0.622	525.59	0.632	525.55	0.642
0.6771	553.81	0.568	553.83	0.585	553.85	0.600	553.82	0.615
0.6771	572.62	0.534	598.78	0.521	598.72	0.544	598.75	0.565
1.5235	296.60	0.586	296.62	0.592	296.65	0.598	296.68	0.601
1.5235	320.10	0.616	320.15	0.620	320.17	0.626	320.20	0.632
1.5235	347.75	0.641	347.72	0.646	347.75	0.650	347.79	0.655
1.5235	371.30	0.656	371.32	0.659	371.35	0.665	371.40	0.668
1.5235	396.98	0.663	397.39	0.667	397.48	0.673	397.51	0.677
1.5235	417.21	0.664	417.22	0.668	417.22	0.675	417.28	0.679
1.5235	448.24	0.658	448.28	0.664	448.31	0.671	448.35	0.674
1.5235	468.83	0.645	468.94	0.655	468.97	0.663	468.99	0.668
1.5235	498.82	0.628	498.87	0.636	498.91	0.645	498.95	0.652
1.5235	526.79	0.584	526.84	0.595	526.87	0.608	526.89	0.620
1.5235	552.27	0.557	552.31	0.576	552.34	0.587	552.36	0.600
1.5235	572.78	0.522	590.43	0.511	590.45	0.532	590.48	0.554
2.598	294.65	0.576	294.70	0.584	294.66	0.584	294.61	0.588
2.598	321.49	0.608	321.50	0.612	321.55	0.616	321.50	0.620
2.598	345.60	0.628	345.62	0.632	345.65	0.636	345.68	0.640
2.598	373.27	0.644	373.30	0.648	373.35	0.652	373.38	0.656
2.598	396.35	0.651	396.37	0.655	396.41	0.660	396.38	0.662
2.598	417.54	0.653	417.55	0.658	417.60	0.661	417.65	0.667
2.598	445.35	0.646	445.36	0.650	445.40	0.658	445.43	0.663
2.598	469.12	0.636	469.15	0.640	469.20	0.648	469.19	0.656
2.598	499.47	0.614	449.45	0.622	499.40	0.631	499.38	0.639
2.598	524.05	0.587	524.08	0.599	524.01	0.609	524.09	0.619
2.598	552.73	0.545	552.76	0.560	552.72	0.576	552.76	0.584
2.598	572.45	0.508	589.75	0.498	589.70	0.498	589.72	0.541
4.063	298.15	0.570	298.17	0.574	298.21	0.578	298.25	0.582
4.063	322.29	0.598	322.32	0.600	322.36	0.604	322.45	0.608
4.063	348.74	0.620	348.78	0.621	348.50	0.626	348.54	0.628
4.063	375.30	0.632	375.33	0.635	375.38	0.640	375.45	0.642
4.063	399.09	0.638	399.11	0.641	399.31	0.647	399.34	0.649
4.063	418.37	0.637	418.39	0.642	418.45	0.648	418.51	0.651
4.063	450.25	0.631	450.38	0.637	450.31	0.644	450.36	0.648
4.063	469.97	0.622	470.03	0.630	470.11	0.637	470.04	0.642
4.063	499.25	0.602	499.37	0.610	499.42	0.619	499.75	0.626
4.063	528.34	0.571	528.41	0.582	528.45	0.594	528.57	0.601
4.063	554.45	0.532	554.49	0.547	554.38	0.562	554.41	0.574
4.063	572.38	0.497	589.12	0.488	589.40	0.510	589.35	0.530

gap. The values of T_{ave} were accepted as experimental temperatures.

The thermal conductivity of $H_2O + Ca(NO_3)_2$ solutions was measured as a function of temperature at constant pressure for various compositions. In Figure 1, the temperature dependence of the measured values of thermal conductivity for the $H_2O + Ca(NO_3)_2$ solutions along various isobars and compositions is shown on each isopleth−isobaric curve. The thermal conductivity shown its maximum value at temperatures between (406 and 440) K depending on pressure and concentration. For pure water, this maximum occurs at temperatures between (409 and 421) K as pressure changing between (20 and 60) MPa. The thermal conductivity maximum is largely affected by composition and pressure. For example, for molality of 0.6771 mol·kg^{-1} at pressures of 10 MPa; the maximum in the thermal conductivity occurs at temperature of about 415 K and shifts to the high temperature of about 425 K as composition changes. At the same isobar (10 MPa), the maximum of thermal conductivity for pure water occurs at a temperature of 405 K.

Figure 2a,b shows the results of the thermal conductivity measurements for $H_2O + Mg(NO_3)_2$ solutions as a function of pressure. The thermal conductivity increases almost linearly as the pressure increases in the temperature range up to 593.15 K and at pressures up to 40 MPa. The composition dependences of the measured thermal conductivities for $H_2O + Ca(NO_3)_2$ solutions for all isotherms and one isobar (20 MPa) are shown in Figure 3a,b. The thermal conductivity of the solution monotonically decreases with composition. As one can see from Figure 3a,b, the composition dependence of the thermal conductivity exhibits a small curvature at high compositions (m > 1 mol·kg^{-1}).

Correlation

Because of the lack of theoretical background on the temperature, pressure, and composition, dependency of the thermal conductivity for aqueous salt solutions, empirical and semispherical correlation equations, and prediction techniques

Table 5. Experimental Thermal Conductivities, Pressures, Temperatures, and Molality of $H_2O + Ba(NO_3)_2$ Solutions

	P/MPa = 10		P/MPa = 20		P/MPa = 30		P/MPa = 40	
m	T	λ	T	λ	T	λ	T	λ
mol·kg^{-1}	K	W·m^{-1}·K^{-1}	K	W·m^{-1}·K^{-1}	K	W·m^{-1}·K^{-1}	K	W·m^{-1}·K^{-1}
0.0781	296.95	0.612	298.12	0.619	296.93	0.626	297.34	0.633
0.0781	317.23	0.635	317.54	0.642	318.01	0.648	317.76	0.654
0.0781	336.34	0.654	335.98	0.660	336.12	0.665	336.74	0.671
0.0781	351.09	0.665	351.79	0.671	352.22	0.677	352.07	0.682
0.0781	378.56	0.681	378.23	0.687	378.97	0.691	378.43	0.697
0.0781	397.53	0.687	397.14	0.693	397.93	0.698	397.23	0.704
0.0781	412.27	0.689	412.88	0.695	412.99	0.701	413.15	0.706
0.0781	436.67	0.686	436.03	0.693	436.81	0.700	436.99	0.706
0.0781	457.86	0.679	457.32	0.687	457.78	0.694	457.12	0.702
0.0781	477.32	0.667	476.94	0.676	476.11	0.685	476.56	0.694
0.0781	491.16	0.656	491.77	0.666	492.15	0.676	492.33	0.686
0.0781	520.49	0.627	521.10	0.639	520.67	0.652	520.22	0.664
0.0781	526.45	0.607	536.76	0.621	536.77	0.634	537.11	0.648
0.0781	552.08	0.584	552.65	0.599	553.04	0.615	553.89	0.630
0.0781	567.08	0.554	588.27	0.548	587.62	0.560	587.32	0.583
0.1594	296.97	0.611	297.14	0.617	296.43	0.624	296.78	0.630
0.1594	317.90	0.634	318.21	0.640	317.66	0.646	317.55	0.652
0.1594	336.45	0.653	336.67	0.658	336.10	0.664	336.34	0.669
0.1594	352.78	0.665	352.55	0.670	352.69	0.675	352.75	0.684
0.1594	377.73	0.679	378.42	0.685	378.23	0.692	378.39	0.696
0.1594	397.90	0.686	398.32	0.691	397.58	0.697	397.11	0.703
0.1594	412.80	0.687	412.93	0.693	413.17	0.699	413.02	0.705
0.1594	437.02	0.685	437.11	0.692	437.04	0.698	437.22	0.705
0.1594	457.67	0.677	458.21	0.685	457.91	0.693	457.66	0.701
0.1594	476.05	0.665	476.98	0.675	477.11	0.684	477.56	0.693
0.1594	493.21	0.655	493.45	0.665	492.07	0.675	520.92	0.663
0.1594	521.23	0.625	520.93	0.638	521.18	0.650	536.31	0.647
0.1594	536.78	0.582	537.11	0.619	536.81	0.633	552.83	0.629
0.1594	567.23	0.553	553.85	0.598	553.31	0.614	587.54	0.580
0.1594			589.24	0.537	588.03	0.561		
0.2442	297.14	0.610	297.81	0.616	298.10	0.622	298.07	0.628
0.2442	317.67	0.633	318.05	0.639	317.97	0.644	318.01	0.650
0.2442	336.48	0.651	336.55	0.657	336.71	0.662	336.85	0.667
0.2442	351.67	0.663	351.87	0.669	352.08	0.674	351.98	0.679
0.2442	378.14	0.678	378.57	0.684	378.88	0.689	378.90	0.695
0.2442	397.27	0.684	397.73	0.690	397.85	0.692	397.77	0.701
0.2442	412.31	0.686	412.84	0.692	413.02	0.698	412.91	0.704
0.2442	436.92	0.683	437.02	0.690	436.98	0.697	457.80	0.700
0.2442	457.64	0.676	457.34	0.684	457.92	0.692	477.57	0.692
0.2442	477.89	0.664	477.21	0.673	477.35	0.683	491.92	0.685
0.2442	491.86	0.653	492.33	0.664	492.07	0.674	521.12	0.662
0.2442	520.36	0.624	520.99	0.637	521.08	0.649	537.06	0.646
0.2442	536.28	0.604	536.64	0.618	536.89	0.632	552.84	0.628
0.2442	552.45	0.581	552.67	0.596	552.78	0.612	587.84	0.600
0.2442	567.01	0.551	587.14	0.536	587.63	0.563		
0.3327	297.93	0.609	298.08	0.614	297.99	0.620	298.12	0.625
0.3327	317.90	0.632	317.89	0.637	317.78	0.642	317.53	0.647
0.3327	336.96	0.650	336.84	0.655	336.70	0.660	336.40	0.666
0.3327	351.75	0.662	351.54	0.667	351.49	0.672	351.98	0.677
0.3327	378.90	0.677	378.55	0.682	378.60	0.688	379.82	0.693
0.3327	397.67	0.683	397.60	0.688	397.58	0.694	397.47	0.700
0.3327	412.87	0.684	412.73	0.691	412.68	0.697	412.50	0.703
0.3327	436.58	0.681	436.68	0.689	436.55	0.696	436.43	0.704
0.3327	457.39	0.674	457.55	0.683	457.61	0.691	457.88	0.699
0.3327	477.71	0.663	477.88	0.672	477.72	0.682	477.93	0.691
0.3327	491.77	0.652	491.64	0.662	491.78	0.672	491.94	0.683
0.3327	521.03	0.622	521.11	0.635	521.07	0.648	520.86	0.661
0.3327	536.94	0.603	537.02	0.616	536.89	0.631	536.55	0.645
0.3327	552.89	0.579	552.70	0.595	552.58	0.611	552.40	0.627
0.3327	567.30	0.550	587.44	0.547	587.34	0.567	587.20	0.580

and using the literature are shown. The results of the (λ, P, T, and m) measurements for $H_2O + Mg(NO_3)_2$, $H_2O + Ca(NO_3)_2$, and $Ba(NO_3)_2$ solutions were represented by

$$\lambda = \sum_{i=0}^{1}\sum_{j=0}^{1}\sum_{k=0}^{2} \alpha_{ijk} m^i P^j t^k \qquad (2)$$

where λ is the thermal conductivity of the solution (W·m^{-1}·K^{-1}), t is the temperature in °C, P is the pressure in MPa, and m is the amount substance per unit mass (mol·kg^{-1}). At high concentrations (m > 1 mol·kg^{-1}), nonlinear terms for the composition dependence in eq 2 have to be included. Equation 2 describes the thermal conductivity of this aqueous salt solutions with an accuracy that does not exceed their experimental uncertainty. The average absolute deviation between measured and calculated values with eq 2 was 0.7 %. The coefficients of eq 2 have been exclusively determined in order to minimize the mean quadratic deviation of the fitted experi-

Table 6. Parameters α_{ijk} of Equation 2

$i = 0$			$i = 1$		
k	$j = 0$	$j = 1$	k	$j = 0$	$j = 1$
		$H_2O + Mg(NO_3)_2$			
0	0.5719266	$-1.603913\cdot10^{-3}$	0	$6.372559\cdot10^{-4}$	$6.791729\cdot10^{-7}$
1	$1.605713\cdot10^{-3}$	$1.288042\cdot10^{-7}$	1	$-3.859074\cdot10^{-6}$	$-5.876942\cdot10^{-8}$
2	$-5.790197\cdot10^{-6}$	$2.268679\cdot10^{-10}$	2	$2.524689\cdot10^{-8}$	$1.312671\cdot10^{-10}$
		$H_2O + Ca(NO_3)_2$			
0	0.5687511	$-1.079345\cdot10^{-3}$	0	$7.993156\cdot10^{-4}$	$-4.084202\cdot10^{-6}$
1	$1.672234\cdot10^{-3}$	$-1.768822\cdot10^{-6}$	1	$-6.348608\cdot10^{-6}$	$1.202095\cdot10^{-8}$
2	$-5.993841\cdot10^{-6}$	$5.842346\cdot10^{-9}$	2	$3.184084\cdot10^{-8}$	$-6.31676\cdot10^{-11}$
		$H_2O + Ba(NO_3)_2$			
0	0.5676432	$6.103516\cdot10^{-6}$	0	$9.235476\cdot10^{-4}$	$-4.089176\cdot10^{-5}$
1	$1.666877\cdot10^{-3}$	$-8.773804\cdot10^{-6}$	1	$-7.178322\cdot10^{-6}$	$5.197899\cdot10^{-7}$
2	$-5.94882\cdot10^{-6}$	$2.126326\cdot10^{-8}$	2	$3.378216\cdot10^{-8}$	$-1.2883776\cdot10^{-9}$

mental thermal conductivity values. The derived values of the coefficients α_{ijk} in eq 2 for this aqueous salt solution are given in Table 6. Equation 2 is valid in the temperature range from (290.15 to 595.15) K, at pressures up to 40 MPa, and for composition up to 4 mol·kg^{-1}.

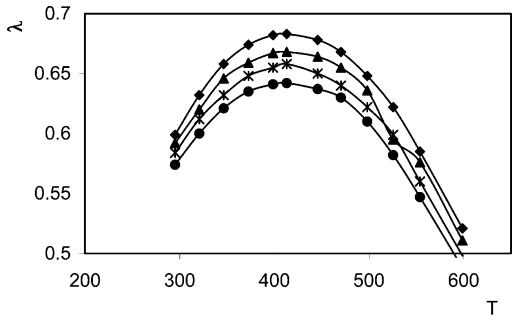

Figure 1. Measured values of thermal conductivity of $H_2O + Ca(NO_3)_2$ solutions as a function of temperature for $P = 20$ MPa and various compositions: ■, 0.6771 mol·kg^{-1}; ▲, 2.598 mol·kg^{-1}; *, 1.5235 mol·kg^{-1}; ●, 4.063 mol·kg^{-1}.

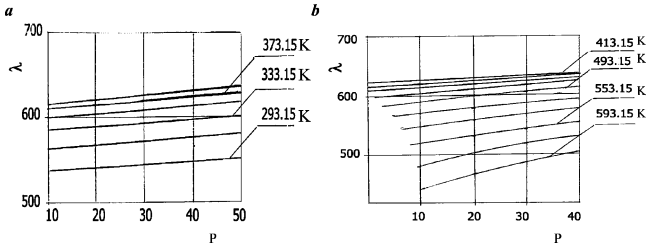

Figure 2. Measured values of thermal conductivity of $H_2O + Mg(NO_3)_2$ solutions as a function of pressure for various temperatures and $m = 4.504$ mol·kg^{-1}.

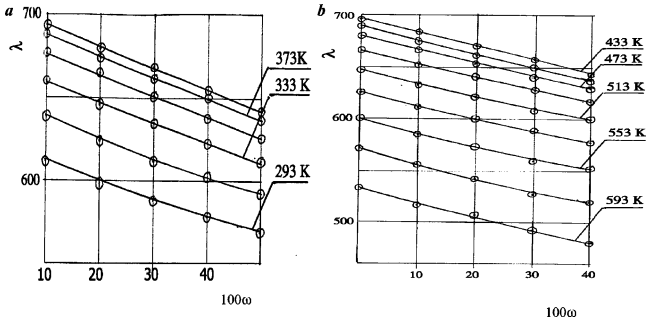

Figure 3. Measured values of thermal conductivity of $H_2O + Ca(NO_3)_2$ solutions as a function of composition along one pressure (20 MPa) and for various temperatures.

Conclusion

The thermal conductivities of five aqueous $Mg(NO_3)_2$, $Ca(NO_3)_2$, and $Ba(NO_3)_2$ solutions have been measured with a coaxial cylinder (steady-state) technique. Measurements were made at five isobars (0.1, 10, 20, 30, and 40) MPa for all solutions. The range of the temperature was (293.13 to 591.06) K. The total uncertainty of thermal conductivity, pressure, temperature, and composition measurements were estimated to be less than 2 %, 0.05 %, 30 mK, and 0.02 %, respectively. The temperature, pressure and concentration dependencies of thermal conductivity were compared with data and correlations reported in the literature. The reliability and accuracy of the experimental method were confirmed with measurements on pure water. The experimental and calculated values of thermal conductivity for pure water from IAPWS[10] formulation show excellent agreement within their experimental uncertainties (AAD within 0.44 %). The correlation equation for thermal conductivity was obtained as a function of temperature, pressure, and composition by a least-squares method from the experimental data. The AAD between measured and calculated values of thermal conductivity for solutions from this correlation equation was 0.7 %. The measured thermal conductivity values of solutions were compared with the data reported in the literature by other authors. Good agreement {deviation within (0.72 to 1.25) %} is found between the present measurements and the data sets reported by other authors in the literature.

Literature Cited

(1) Azizov, N. D. Thermal conductivity of aqueous solutions of Li_2SO_4 and $Zn(NO_3)_2$. *Russ. High Temp.* **1999**, *37*, 649−651.

(2) Akhundov, T. C.; Iskenderov, A. I.; Akhmedova, L. A. Thermal conductivity of aqueous solutions of $Ca(NO_3)_2$. *Izv. Vuzov. Ser. Neft Gas* **1994**, *3*, 49−52.

(3) Akhundov, T. C.; Iskenderov, A. I.; Akhmedova, L. A. Thermal conductivity of aqueous solutions of $Mg(NO_3)_2$. *Izv. Vuzov. Ser. Neft Gas* **1995**, *1*, 56−58.

(4) Abdulagatov, I. M; Magomedov, U. M. Thermal conductivity measurements of aqueous $SrCl_2$ and $Sr(NO_3)_2$ solutions in the temperature range between 293 and 473 K at pressures up to 100 MPa. *Int. J. Thermophys.* **1999**, *20*, 187−196.

(5) Abdulagatov, I. M; Magomedov, U. B. Thermal conductivity of aqueous solutions of NaCl and KCl at high pressures. *Int. J. Thermophys.* **1994**, *15*, 401−413.

(6) Abdulagatov, I. M; Akhmedova-Azizova, L. A.; Azizov, N. D. Thermal conductivity of aqueous $Sr(NO_3)_2$ and $LiNO_3$ solutions at high temperatures and high pressures. *J. Chem. Eng. Data* **2004**, *49*, 688−703.

(7) Abdulagatov, I. M; Akhmedova-Azizova, L. A.; Azizov, N. D. Thermal conductivity of binary aqueous NaBr and KBr and ternary H_2O + NaBr solutions at temperatures from (294 to 577) K and pressures up to 40 MPa. *J. Chem Eng. Data* **2004**, *49*, 1727−1737.

(8) Akhmedova-Azizova, L. A.; Guseinov, K. D. Heat conductivity of solutions the main components of working fluids of the thermal power

industry. *Conference Proceedings, Second International Conference on Technical and Physical Problems in Power Engineering*, Tabriz, Iran, 2004.

(9) Abgulagatov, J. M.; Magomedov, U. B. Thermal conductivity of pure water and aqueous $SrBr_2$ solutions at high temperatures and high temperatures and high pressures. *High Temp.*−*High Pressures* **2004**, *35*/*36*, 149−168.

(10) Kestin, J.; Sengres, J. V.; Kamgar-Parsi, B.; Levelt Sengres, J. M. H. Thermophysical properties of fluid H_2O. *J. Phys. Chem. Ref. Data* **1984**, *13*, 175−189.

(11) Gershuni, G. Z. Thermal convection in the space between vertical coaxial cylinders. *Dokl. Akad. Nauk USSR* **1952**, *86*, 697−698.

(12) Healy, J.; de Groot, J. J.; Kestin, J. The theory of the transient hot-wire method for measuring thermal conductivity. *Phys. C* **1976**, *82*, 392−408.

(13) Ramires, M. L.; Nieto de Castro, C. A.; Nagasaka, Y.; Nagashima, A.; Assael, M. J,; Wakeham, W. A. Standard reference data for the thermal conductivity of water. *J. Phys. Chem. Ref. Data* **1995**, *24*, 1377−1381.

Received for review September 28, 2005. Accepted January 17, 2006.

JE050393N